PHYSICAL *AND* CHEMICAL CHARACTERISTICS OF SFE FIRE SUPPRESSANT ATMOSPHERES: COMPARISON OF SMALL WITH LARGE SCALE LABORATORY ATMOSPHERES.

E.C. Kimmel*, E.A. Smith", J.E.Reboulet*, B.H. Black**, RS. Sheinson°
and RL. Carpenter°°

INTRODUCTION

   SFE is a fine, dry powder aerosol fire extinguishant which is currently undergoing evaluation as a possible replacement for halon **1301** total flooding agent used in some Naval systems. The results of an investigation conducted at the Naval Research Laboratory / Chesapeake Bay Detachment (NRL/CBD) of SFE fire extinguishment efficacy have been reported (1). However, comprehensive evaluation of any possible halon replacement candidate, including SFE, requires assessment of it's potential inhalation toxicity. Findings of a pilot investigation of **SFE** (SFE formulation **A**) inhalation toxicity **(2)** conducted at the Naval Medical Research Institute Detachment: Toxicology (NMRI/TD) demonstrated a need for further investigation of potential toxicity, **as** well **as,** a more complete characterization of SFE atmospheres as deployed in field testing conditions.

   SFE aerosols are pyrotechnically generated by ignition of the bulk **SFE.** SFE pyrolysis is self perpetuating and produces transient pressure and thermal pulses which could feasibly obfuscate inhalation toxicity evaluations. Hence, for toxicity evaluations a system was designed in which the SFE could be ignited in one portion of the system for rapid dissipation of the pressure and thermal pulse prior to transport of the atmosphere produced into a standard inhalation exposure chamber **(3).** This procedure differs from the fire extinguishment testing scenario used at NRL/CBD in which **SFE** is ignited within the test chamber itself and which more closely simulates present deployment methods and conditions. Although the basic pyrotechnical methods of SFE aerosol generation are same between the two test conditions, some fundamental system differences suggested the need for a more extensive characterization of the aerosol and gas/vapor phases of the both test atmospheres. The present investigation was undertaken to facilitate extrapolation of results between toxicity testing and fire extinguishment testing atmospheres.

....
*   ——Centers, Inc. at NMRI/TD
**   Geo-Centers, Inc at NRL
° **Naval** Research **Laboratory (NRL)**
°° **Naval Medical** Research **Institute Detachment** Toxicology (NMRI/TD)
NMRI/TD, Bldg. 433 *Area* **B, Wright-Patterson AFB, OH 45433**

METHODS

SFE

The SFE (Formulation A) tested in both systems was obtained from the Spectrex, Inc., the U.S. subsidiary of an Isreali company Spectronix, Ltd. The composition of SFE is proprietary. Experiments in both systems were conducted at two nominal concentrations in which either 50 or 80 g of test material per m^3 of chamber volume was ignited. The volume of the NRL/CBD facility has been reported at 56 m^3 and the volume of the inhalation exposure chamber and system used at NMRI/TD was 0.7 m^3.

Atmosphere (aerosol) Generation

The aerosol generators used in the 56 m^3 chamber test system have been previously described in detail (1). The aerosol generator used in the 0.7 m^3 test system was manufactured out of two sections of 3 in. diameter schedule 80 stainless steel pipe [Figure 1 - (4)]. The lower section (h $\cong$ 7.6 cm) was flanged and bolted to an upper flanged section of pipe (h $\cong$ 20.3 cm). A stainless steel fritted metal plate (0.3 cm thick) was fitted between the flanges. The lower section included an 1/8 in. compression fitting through which metered air flow was introduced to facilitate transport the SFE combustion atmosphere to the exposure chamber. The upper section of the generator was fitted with 1/16th in. and 1 in. compression fittings through which a thermocouple and an insulator/ electrode assembly were secured. A 5 cm diameter ceramic boat was placed in the bottom of the upper plenum (on the fritted plate) in which nichrome wire (connected to the electrodes) was coiled. Weighed portions of 100 g SFE pellets were placed directly on the coils. The top of the generator/igniter assembly was a portion of 3 in. fnpt coupler welded to the pipe to accept a threaded adapter to 3 in. diameter aluminum duct for transport to the exposure chamber (total length $\cong$ 2.5 m). The SFE was by application of an 18 v, 6 amp current through a length of 26 AWG nichrome with 3 ohm resistance ($\cong$ 28 cm) which produced the $\cong$ 500°C temperature required to start pyrolysis of the SFE. The 3 in. duct ($\cong$ 2.5 m) also served to dissipate the thermal energy. Generator temperatures reached 1100$\pm$ 100"C yet chamber temperatures remained at 22 to 24 "C.

Test Chambers

The 0.7 m^3 inhalation exposure chamber was not operated in the mode routinely employed for toxicity experiments. Inhalation exposure chambers normally are run as dynamic (continuous flow) systems with the test atmosphere being generated and mixed continuously with the chamber flow. However, for single event generation such as combustion of SFE a static (non-flowing) operation mode was used. The SFE atmospheres were generated and piped into the exposure chamber during dynamic mode operation; once transport of the test atmosphere was complete the chamber was switched to the static mode via automatic shut off valves at the inlet and exhaust ports. A sight glass fitted into the chamber inlet duct enabled visual determination of cessation SFE pyrolysis. Automated control of system flow and pressure differential assisted chamber filling with no or inconsequential loss of test atmosphere through the chamber exhaust during the dynamic operation/generation phase, while providing control of the generation pressure pulse as

well.   Generator and chamber flow during ignition and filling was 30 - 31 LPM and chamber filling time ranged from 0.75 to 1.0 **min.** at which point static operation was initiated (Figure 1).

Aerosol Analysis

Analytical methods for characterization of the aerosol component of the SFE atmospheres were identical for both test systems. Aerosol mass concentration was determined by gravimetric analysis of particles collected on 37 mm diameter glass fiber filters placed in holders specifically designed for aerosol sampling (Intox Products, Albuquerque, **NM)** through which a known volume of test atmosphere was drawn. Sample flow was measured and controlled with variable area rotameters calibrated to NIST traceable standards. Sample volume was controlled by electronic timing of solenoid valves in the sample lines. Flows and subsequently sample volumes were adjusted for changes in pressure differential across the sampling device. In the $0.7\,m^3$ chamber samples were drawn through short sample probes (**1.2** cm dia) penetrating the chamber wall. Sample velocity and probe design eliminated sample probe aerosol deposition. In the large chamber, the filter holders were located directly within the chamber at the end of separate vacuum lines. Rotameters, solenoids, and electronic timers were used for precision control of sample flow and volume. Filter samples were collected at 1, 15, 30, and 60 min. in the $0.7\,m^3$ chamber and at 1.5, 15, 30 and 60 min. in the $56\ m^3$ chamber. In the small chamber volumes of air equivalent to the sample volume were injected in the chamber exhaust plenum to prevent depressurization of the exposure chamber. Reported concentrations have been adjusted for loss of mass concentration due to previous sample collection.

Mass Median Aerodynamic Diameter (**MMAD)** and the geometric standard deviation (σg) of the aerosol distribution were determined by two methods. Multistage (**8** stages), multijet cascade impactors (Intox Products, Albuquerque, NM) were used to collect samples for gravimetric analysis at time points corresponding to filter sample collections. Sample flows and pressure differentials were controlled in a manner **similar** to filter samples. In the large chamber the impactors also were located w i t h the chamber at the terminus of individual vacuum lines. Aerosol size distribution characteristics also were determined using a laser, time of flight, individual particle analyzer (Model 3300B Aerodynamic Particle Sizer, **TSI,** Inc., St. Paul, MN). The APS was capable of separating the particle distribution into *58* individual size ranges from 0.47 to 30.0 μm diameter particles, thus allowing for a much greater resolution of the particle size distribution. *APS* samples were taken at 1 or 1.5, 15, 30, 45, and 60 min. MMAD and σg determinations were based on impactor samples whereas changes in aerosol distribution shape and modality were based on *APS* samples.

Gas Analysis

CO and CO, concentrations were determined in both the $0.7\,m^3$ and $56\,m^3$ chambers. Chromatographic methods were used to analyze for CO, at the NRL/CBD test site *(56* m^3 chamber) and have been described previously (1). Carbon monoxide concentration in the $56\,m^3$ chamber was measured continuously by wavelength-specific, non-dispersive IR spectrometry (Enviromax 3000, Liston Scientific, Irvine, CA). Wave-length-specific, non-dispersive IR spectrometry was used for both CO and CO, in the $0.7\,m^3$ chamber (Model *865* Beckman

Industries, La Habra, CA). The latter samples were collected at times corresponding to APS samples. Electro-chemical measurement of O_2 concentration in the 56 m^3 chamber was continuous (Enviromax 3000) and on a grab sample basis in the 0.7 m^3 chamber (Model 326RA, Teledyne Analytical Instruments, City of Industry, CA).

Particle morphology

Electrostatic precipitation was used to collect particles for examination by scanning and transmission electron microscopy to determine aerosol particle morphology and composition by x-ray defraction.

Experimental Design

All test periods were 60 minutes. The test schedule was as follows:

> 0.7 m^3 chamber @ 50 g/m^3 - 3 trials
> 0.7 m^3 chamber @ 80 g/m^3 - 4 trials
> 56 m^3 chamber @ 50 g/m^3 - 3 trials
> 56 m^3 chamber @ 80 g/m^3 - 2 trials

RESULTS

Spatial Distribution - 56 m^3 chamber

The 0.7 m^3 inhalation exposure chamber is specifically designed for mixing and even distribution of aerosols within the chamber exposure volume. In the large chamber, mixing and dispersal of the aerosol was accomplished by using a fan during first 1.5 **min.** after ignition of the SFE. A single trial was made at 50/g/m^3 to determine spatial variation within the chamber of aerosol concentration, size distribution and CO, concentration. Measurements were made at 1.5 and 60 min. after ignition of SFE at heights in the chamber of 1, 3, 6 and 11 R. (Figure 2). A maximum difference in initial actual aerosol **mass** concentration of 10.1 to 11.4 g/m^3 at the 1 and 11 ft levels respectively was observed with virtually no difference between any of the levels at 60 **min.** Initial particle MMAD's were 2.9 or 3.0 μm at **all** levels. At 60 min. particle size ranged from a low of 4.4 μm MMAD at the 6 ft level a high of 5.2 μm MMAD at 1 R.. Both the initial and final CO, concentration varied by as much as 3 g/m^3 between levels, fiom 26.5 to 23.4 g/m^3 initially to 11.2 to 13.9 g/m^3 after 60 min.

Aerosol Mass Concentration

Initial, actual aerosol **mass** concentration for both target loads, 50 and 80 g/m^3, was higher in 56 m^3 chamber at 10.2 and 14 g/m^3 respectively vs. 6.3 and 10.0 g/m^3 respectively for the 0.7m^3 chamber. Gravitational settling of particles throughout the test period resulted in final concentrations of 1.7 and 1.2 g/m^3 in the 50 and **80** g/m^3 loads in the 56 m^3 chamber. Final aerosol concentrations in the 0.7 m^3 chamber were 0.7 g/m^3 for both loads (Figure 3). In both chambers and for both target loads decay of aerosol concentration was exponential. Shorter

half-times $(T_{1/2})$ of 15.5 and 16.1 min. were found for the higher target load for the 0.7 and 56 m^3 chambers respectively. $T_{1/2}$ for the low target load was 18.6 and 22.4 **min.** respectively.

Aerosol Size Distribution and Particle **Growth**

The initial MMAD's ranged fiom 2.4 to 3.0 μm for the 56 m^3 chamber - **80 g/m^3** load and 0.7 m^3 chamber - 80 g/m^3 load respectively. The σg's for the particle distributions ranged fiom 1.42 to 2.01 at various times, however average og's were 1.66 to 1.88. Particle growth occurred in both chambers with maximum MMAD being reached at the following times:

0.7 m^3 - 50 g/m^3 - 30 min.
0.7 m^3 - 80 g/m^3 - 15 min.
56 m^3 - 50 g/m^3 - 60 **min.**
56 m^3 - 80 g/m^3 - 30 min.

Growth was more rapid for the higher target load in both chambers and apparently much more rapid in the 56 m^3 chamber (Figure 4). Initially the particle distributions were bimodal with a major mode occurring near the MMAD and minor mode ranging fiom 4 to 17 pm. However, due to gravitational settling the minor mode disappeared after 15 min. in nearly all distributions (Figure 5a and 5b).

CO and CO, Concentration

CO, concentrations in the 56 m^3 chamber were much higher at both target loads than corresponding concentrations in the 0.7 m^3 chamber. The large chamber was not a sealed containment vessel, **as** was the inhalation exposure chamber, thus gas concentration decayed over time due to chamber leak. Initial CO, concentrations for the 50 and 80 g/m^3 loads were 14,475 and 22,200 ppm (26.5 and 40.6 g/m^3) respectively. Final CO, concentrations for the large chamber were 7,100 and 9500 (13 and 17.4 g/m^3) respectively (Figure 6). CO, concentrations in the 0.7 m^3 chamber were steady state at 10,230 to 10,105 ppm for the 50 g/m^3 target load. *CO,* concentrations for the **80 g/m^3** load in the 0.7 m^3 chamber were 9,457 ppm initially to 9,376 ppm at 60 min. However, two distinct CO_2 concentration levels were noted in the small chamber trials at the 80 g/m^3 load, with two trials averaging 12,548 to 12,033 ppm CO, and two trials averaging 6,366 to 6720 ppm CO, (Figure 6). A corresponding difference in CO concentration under these conditions was not observed, *vide **infra.*** Small chamber initial and final CO concentrations were 2,168 and 2,538 ppm (1.9 to 2.9 g/m^3) at the 50 g/m^3 load. At the 80 g/m^3 load initial and final CO concentrations were 6,548 and 6,360 ppm respectively. In the 56 m^3 chamber long sampling lines and a large dead space (in-line filter assembly required to remove particles fiom the sample) in the CO analysis system lead to large sample lag time ($\cong$ 30 min.). Consequently, peak CO concentrations were not seen until the 30 min. sample point. Only moderate concentration decay was observed, which may have been sampling artifact. Peak CO concentrations in the 56 m^3 chamber were, for the 50 and 80 g/m^3 loads respectively, 2,992 and 4,810 ppm. O_2 concentration in the 56 m^3 varied fiom 19.1 to 19.9% and ranged fiom 20.1 to 20.6 % in the 0.7 m^3 chamber.

DISCUSSION

Systems Mass Balance and Comparative Efficiencies

Mass balance calculations, based on peak concentrations, (Figures 7a & 7b) indicate that in the $0.7m^3$ chamber test system **10.7** and **23.4 %** of the mass of SFE ignited, for the **50** and 80 g/m^3 loads, remained unaccounted for by the aerosol , CO, and CO yields. Unaccounted for mass in the **56** m^3 chamber system corresponded to **24.8** and **25 %** of the SFE ignited for the 50 and 80 g/m^3 loads respectively. Thus, irrespective of target load the $0.7m^3$ system used bulk SFE more efficiently than it's **56** m^3 counterpart. However, with respect to aerosol generation **12.3** and **12.4%** of the SFE mass was aerosolized at the **50** and 80 g/m^3 loads in the $0.7m^3$ chamber; whereas aerosolization was **19** and **17.4%** of the SFE mass at the 50 and 80 g/m^3 loads in the **56** m^3 chamber. The average ratio (both target loads) of aerosol formation efficiency the chambers was $56{:}0.7$ m^3 = **1.5:1**. Hence the large system was **50 %** more efficient at aerosol dispersal if not formation. A slightly greater overall efficiency for pyrolysis of **SFE** for the $0.7m^3$ chamber system suggested that transport loss of aerosol and not aerosol production was the cause for the observed difference in aerosol dispersement efficiency. CO, concentration in the $0.7m^3$ system was greater at the lower target load than that of the higher target load. At the 80 g/m^3 level two varieties of **SFE** (both marked formulation A - from the supplier) may have been used. It was observed that the atmosphere produced by the material yielding **0.5** of the expected CO_2 also deposited very **sooty** residue (similar to that seen with ignition of SFE formulation C). Consequently the mass percentages of CO, yield were not similar, at **38.2** and **21.8%** for the **50** and 80 g/m^3 loads respectively. Yield of CO, (using peak concentrations) in the **56** m^3 system were similar at **49.6** and **50.6%** for the **50** and 80 g/m^3 loads. The relative CO, production efficiencies for the systems were $56{:}0.7$ m^3 chambers = 1.3 at 50 g/m^3 load and **2.3** at the **80** g/m^3 load. Thus at the lower target load the **56** m^3 system produces 30 % to 130% more CO, per mass of **SFE** ignited than does the $0.7m^3$ system depending on target load. CO production accounts for **5.9** and **9.5%** of the SFE mass used in the **56** m^3 system at **50** and 80 g/m^3 loads. CO yield in the $0.7m^3$ system was **6.5** and **6.9%** for the **50** and 80 g/m^3 loads respectively. Therefore CO production efficiency ratio for the systems was $56{:}0.7$ = **0.8** at 50 g/m^3 and **1.5** at 80 g/m^3 targets. Differences of Carbon combustion efficiency between the generation systems was responsible for the discrepancy in relative CO and CO, concentration between the test systems.

Aerosol Growth

For aerosols with $\cong 3.0\,\mu m$. MMAD's and $\sigma g.s$ of **1.7** the high initial mass concentrations observed in the study of **14, 10.2, 10.0** and **6.3** g/m^3 [(assuming a particle density of 2.0 g/cm^3 for SFE - (4)] the corresponding particle number concentrations were **1.78x 10^6**, **1.30x 10^6, 1.27x 10^6** and 0.8 x 10^6 particles/cm^3 . Aerosols with a number concentration of 1.0 x 10^6 particles/cm^3 have a number concentration $T_{,,}$ of $\cong$ **33 min**. due to coagulation and agglomeration of particles, without loss of total mass in the particle distribution (5). Therefore, part of the particle growth and shift of the particle distribution toward larger MMAD could be attributed to this phenomena. Electron micrography and X-ray dispersive analysis showed that the SFE aerosol particles were cubiodal crystals composed ($\cong$ **97.0%**) of KCl. Given this

composition the particles were expected to be hygroscopic and highly soluble. The apparent acceleration of particle growth in the $56\,m^3$ chamber is most likely a result of increased adsorption of water due to RH% differences, **30 & 100%** for the 0.7 and 56 m' chambers respectively. Particle growth due to agglomeration was greater for the higher load. However, regardless of particle concentration hygroscopic growth exerted the greatest influence on **shifts** of aerosol distribution MMAD. Interestingly, the shift of the particle size distribution toward larger MMAD (Figures 5a & 5b) continued despite early gravitational settling of the larger particles as shown by the disappearance of the minor mode.

System Atmosphere Differences and Particle Growth: Toxicity Implications

An average (both load levels) relative aerosol dispersal efficiency ratio of $\cong$ **1.5** for the **56** m^3 chamber conditions **vs..** the 0.7 m^3 conditions would favor a comparable 1.5 ratio for total aerosol mass deposition in lungs at a given minute ventilation (Ve). For example at the **80** g/m load level an individual with a resting Ve of 7 LPM (assuming 0.9 deposition fraction, *vide infra*) exposed to the 56 m^3 chamber atmosphere, at peak aerosol concentration of 14.0 g/m³ , would have **9.8** x 10^{-2} **grams/min**. total lung deposition rate. The same individual exposed to the **0.7** m^3 chamber atmosphere, at peak aerosol concentration of 10.0 g/m³ , would have 7.0 x 10^{-2} g/min. total lung deposition rate. At the 50 g/m³ load the corresponding deposition rates would be 7.1 x 10^{-2} g/min and 4.4 x 10^{-2} **g/min**.

Based on the current **ICRP** (International Commission on Radiation Protection) human particle deposition curves (6) the particle size increases observed in all experimental conditions would increase total lung deposition (TL) - (Figure **8).** One μm increases in MMAD in the 0.7 m^3 chamber seen for the 50 and **80** g/m³ loads correspond to increases in total lung deposition of 5 and 3 %. In the 56 m^3 chamber **2** μm increase of MMAD would result in a **7%** increase in TL while an increase of **MMAD** of **3.9** μm at the **80** g/m³ load would result in a 20 % increase in TL. Particle growth induced deposition changes would be greater for deposition in various regions of the lung. In the naso-oro-phayngeal (NP) region particle deposition would increase by as little as **8%** (0.7 m^3 - 80 g/m³) to as much as 45 % **(56** m^3 - **80** g/m³) - (Figure 9). Tracheobronchial (TB) region deposition (7) would increase by 6 % at either target load in the 0.7 m^3 chamber and by **14** and **33%** in 56 m^3 chamber at 50 and **80** g/m³ respectively (Figure 10). With initial MMAD's and magnitude of particle growth observed in the present study pulmonary (P) regional deposition would decrease. In the 0.7 m^3 chamber P deposition would decrease 17 and 16% at the low and high loads. Decreases P region fractional deposition would be greater in the 56 m^3 chamber at 26 and 44 %. These large decreases in the P region would have greater significance for less soluble aerosols because of the relatively slower clearance from this compartment. However, since SFE particles are highly soluble shifts in regional deposition pattern and thus clearance and retention pattern assume secondary relevance to TL deposition changes, primarily because of circumvention of normal clearance mechanisms.

Breathing 1% (10000 ppm) atmospheres of *CO,* has been shown to increase Ve from 7 to 9 LPM in humans in a few minutes and **2%** atmospheres increase Ve to 11 LPM **(8).** These increases in Ve would result in proportional increases in particle deposition. CO, yield ratios of **1.3** for and **2.3** for the 56 m^3 vs 0.7 m^3 chamber at the 50 and **80** g/m³ loads would result in

proportional increases in particle deposition caused by CO_2 stimulated hyperventilation. At an 80 g/m^3 load the 2.8×10^{-2} g/min. TL deposition difference rate between the 56 and $0.7 m^3$ chamber conditions would increase to a 6.2×10^{-2} g/min. TL deposition difference between the two atmospheres.

Change in the percent baseline carboxyhemoglobin (HbCO) level in man caused by breathing CO can be predicted by the following empirical equation (9), This algorithm was found applicable for humans breathing CO concentrations fiom 90 to 21000 ppm for periods of 20 to 300 min. but with limited reliability at HbCO concentrations above 80 Yo.

$$\Delta [Hb\,CO]\,\% = (CO \times Ve \times t)/\,2.5 \times 10^4,$$
where Ve is LPM, t is min. and CO is ppm. As a point of reference baseline HbCO in non-smokers is 1.3 % and in smokers may vary fiom 5 to 10 %.

Thus at Ve = 7 LPM and exposure to the $0.7 m^3$ chamber 50 and 80 g/m^3 atmospheres for 20 min. the predicted HbCO levels would be $\cong$ 14.4 and 37.4% . In the 56 m^3 chamber corresponding HbCO levels would be 20.6 and 27.5%, if concentration decay did not occur. Although this simple mathematical description is adequate for rudimentary estimates of HbCO formation and homeostasis, further investigation which includes measurement of pertinent physiological responses to CO exposure are required. The potential differences of physiological response fiom exposure to steady state concentrations of CO and CO_2 and exposure to atmospheres with decaying CO and CO, concentrations require further examination.

With exception of potential CO concentration effects on HbCO the 0.7 m^3 at the higher target load, characteristics of the SFE atmospheres generated in the larger test chamber appear to pose a higher relative potential inhalation toxicity risk.

REFERENCES

1. **Sheinson, RS, HG Eaton, RG Zalosh, BH Black, R Brown, H Burchell, GSalmon and WD Smith. 1994.** Intermediate Scale Fire Extinguishment by Pyrogenic Solid Aerosol. *Proceedings of Halon Options Technical Working Conference.* May 3 - 5, Albuquerque, NM.

2. **Smith EA, EC Kimmel, LE Bowen, JE Reboulet and RL Carpenter. 1994.** The Toxicological Assessment of Fire Suppressant and Potential Substitute for Ozone Depleting Substances. *Proceedings of Halon Options Technical Working Conference.* May 3 - 5, Albuquerque, NM.

3. **Kimmel EC and KL Yerkes. 1990.** Design, Performance and Fluid Mechanics of a Small Animal, Whole-body Inhalation Exposure Chamber. In: 1989 Toxic Hazards Research Unit Annual Report. Armstrong Aerospace Medical Research Laboratory, Wright-Patterson AFB, OH. *(AAMRL-TR-90-051).*

4. **Kimmel EC, EA Smith, LE Bowen, JE Reboulet and RL Carpenter. 1994.** physical and Chemical Characterization of Aerosols of Three Formulations of SFE, a Potential Dry Powder

Replacement for Ozone Depleting Fire Suppressants. Presented at *Halon Options Technical Worhng Conference,* May 4, Albuquerque, **NM.**

5. **Hinds WC.** 1982. *Aerosol Technology: Properties, Behavior, and Measurement of Airborne Particles.* John Wiley & Sons, Inc. New York, *NY .*

6. **Raabe OG.** 1989. Experimental Dosimetry: Introduction. In *Extrapolation of Dosimetric Relationships for Inhaled Particles and* Gases. Eds. JC Crapo, ED Smolko, FJ Miller, JA Graham and AW Hayes. Academic Press, Inc. San Diego, CA.

7. **Cheng Y-S and H-C Yeh.** 1981. A Model for Aerosol Deposition in the Human Tracheobronchial Region. *Am. Ind Hyg. Assoc. J.* 42: 771-776.

8. **Dripps RD and JH Comroe Jr.** 1947. The Respiratory and Circulatory Response of Normal Man to Inhalation of 7.6 and 10.4% CO_2 with a Comparison of the Maximal Ventilation Produced by Severe Muscular Exercise, Inhalation of CO_2 and Maximal Voluntary Hyperventilation. *Am. J. Physiol.* 149: 43-51.

9. **Pace N, E Strajman and EL Walker.** 1979. Acceleration of Carbon Monoxide Elimination in Man by **High** Pressure Oxygen. *Science* 111: 652-654.
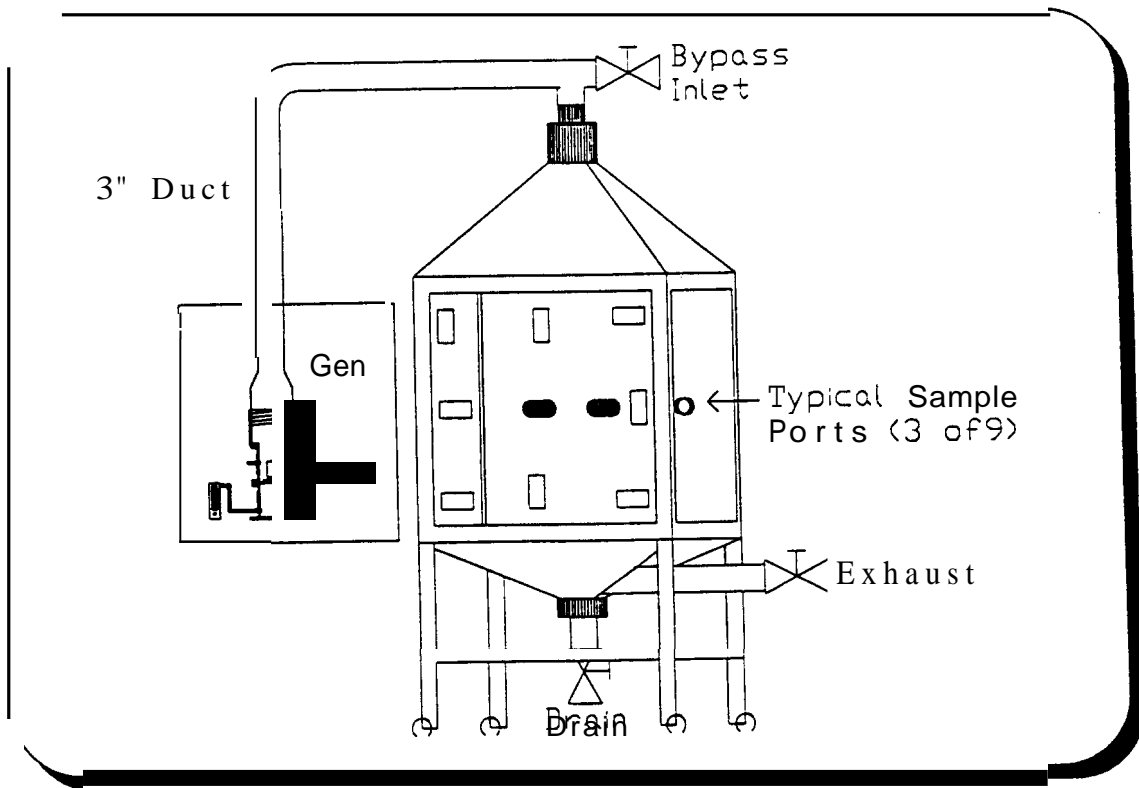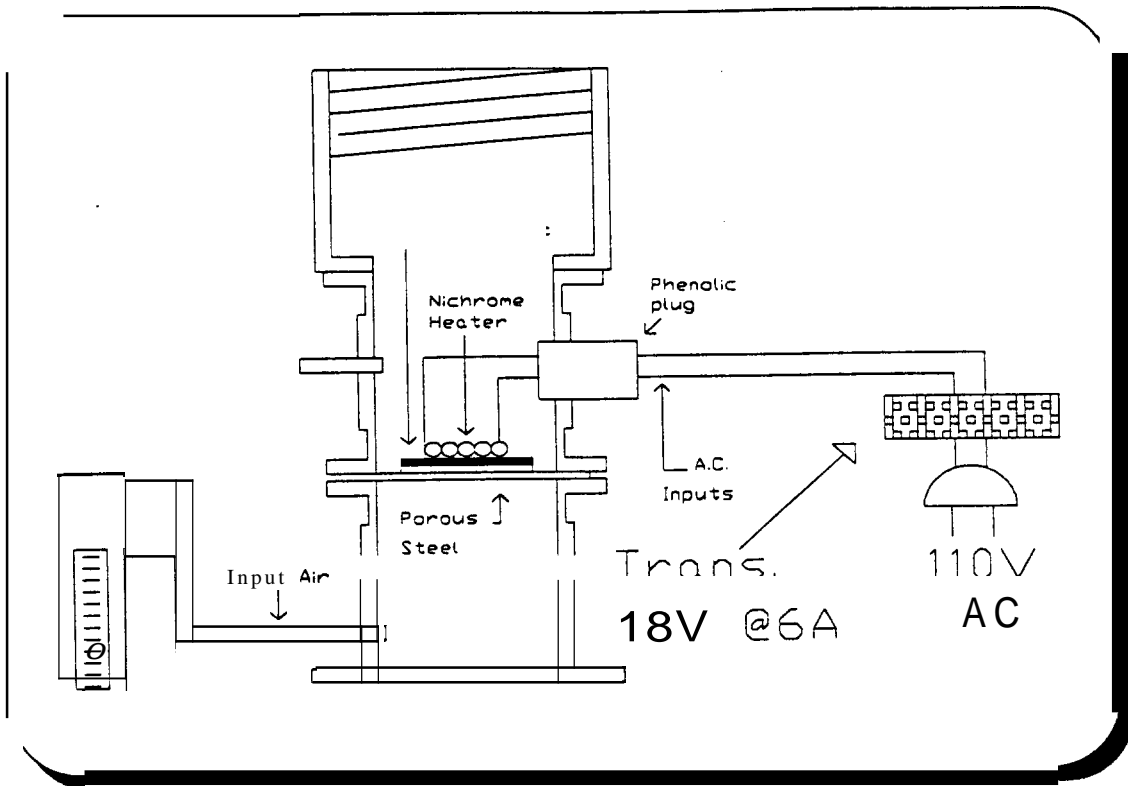
Figure 1. Aerosol Generator & Exposure Chamber - 0.7m^3
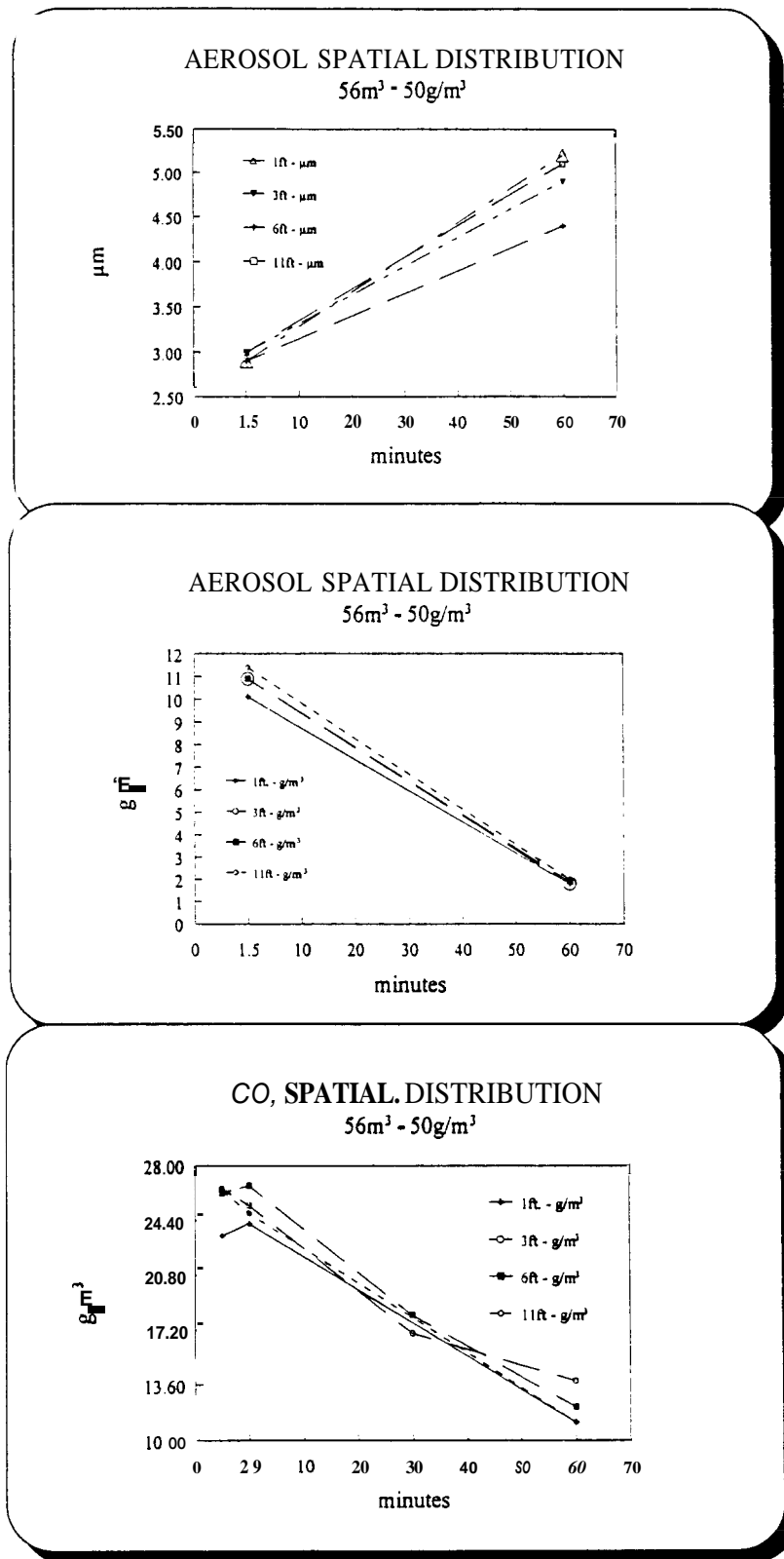
Figure 2. Aerosol/CO$_2$ Distribution in the 56m^3 chamber

AEROSOL CONCENTRATION DECAY
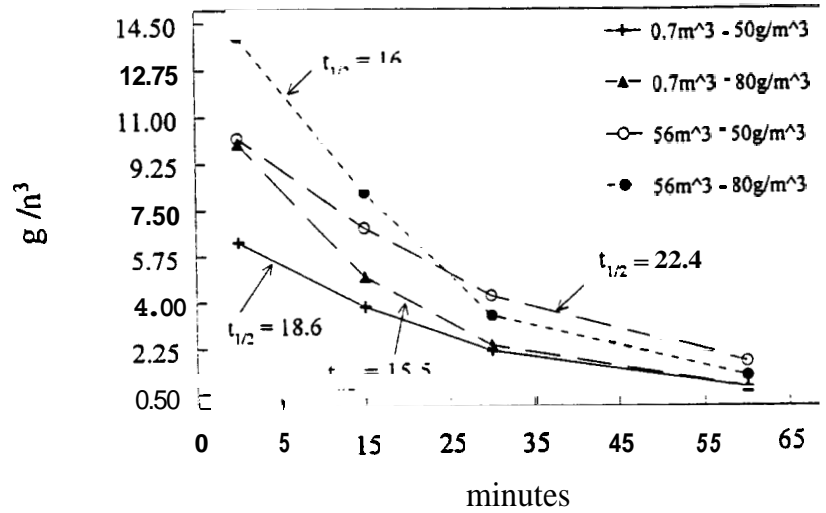
AEROSOL CONCENTRATION DECAY
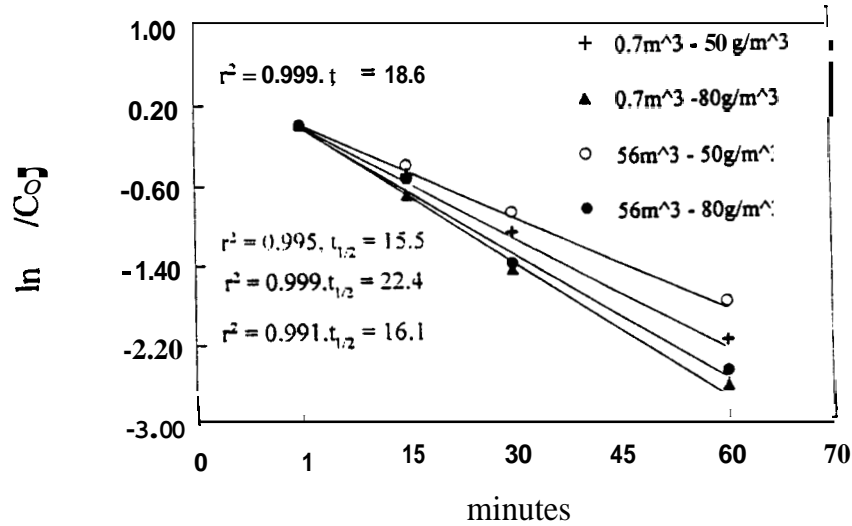
Figure. 3. Aerosol Concentration Decay

PARTICLE GROWTH
0.7 m³ chamber

PARTICLE GROWTH
56m³ chamber
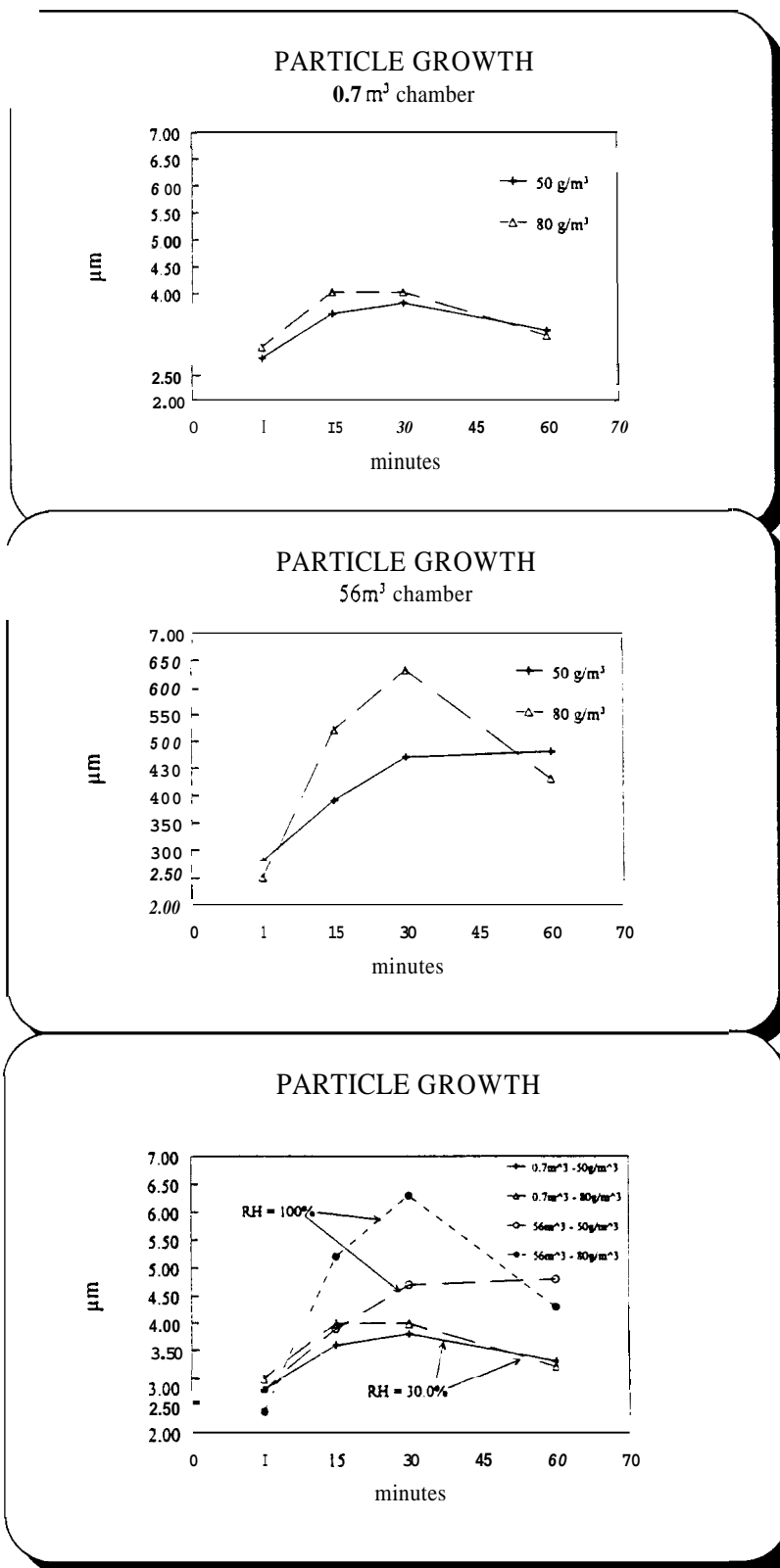
PARTICLE GROWTH

Figure 4. Aerosol Particle Growth

AEROSOL SIZE DISTRIBUTION

$0.7m^3$ chamber - $50gm^3$

AEROSOL SIZE DISTRIBUTION
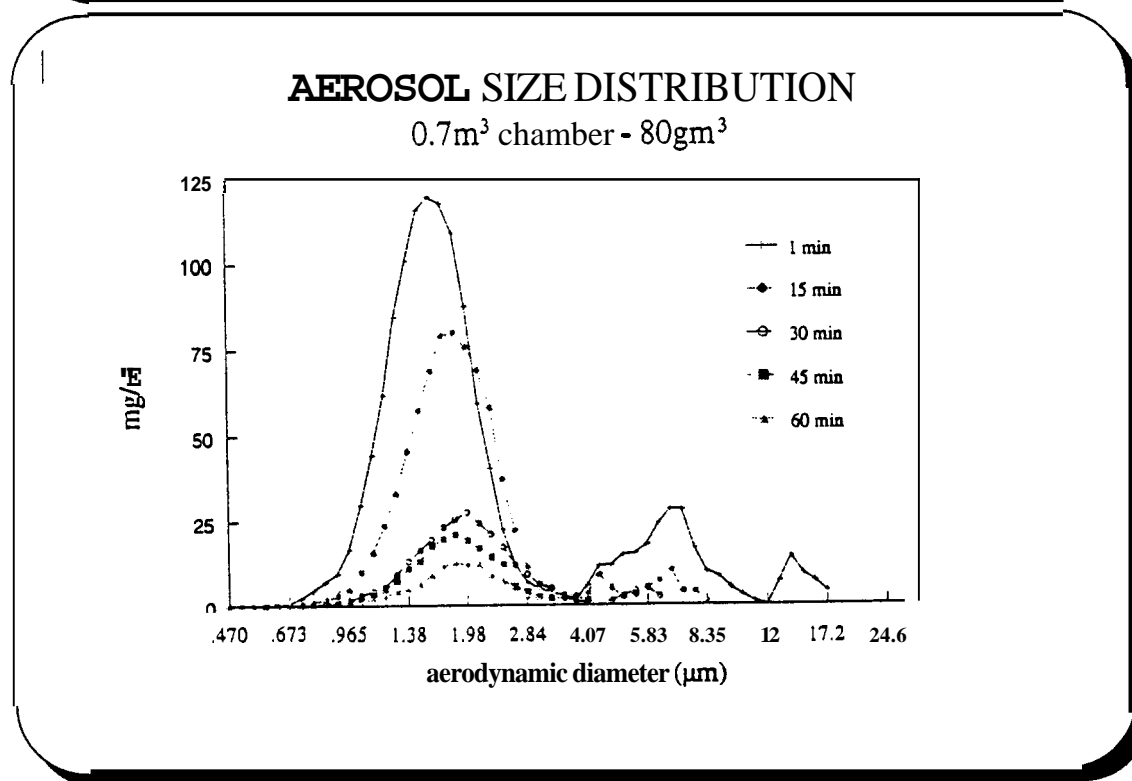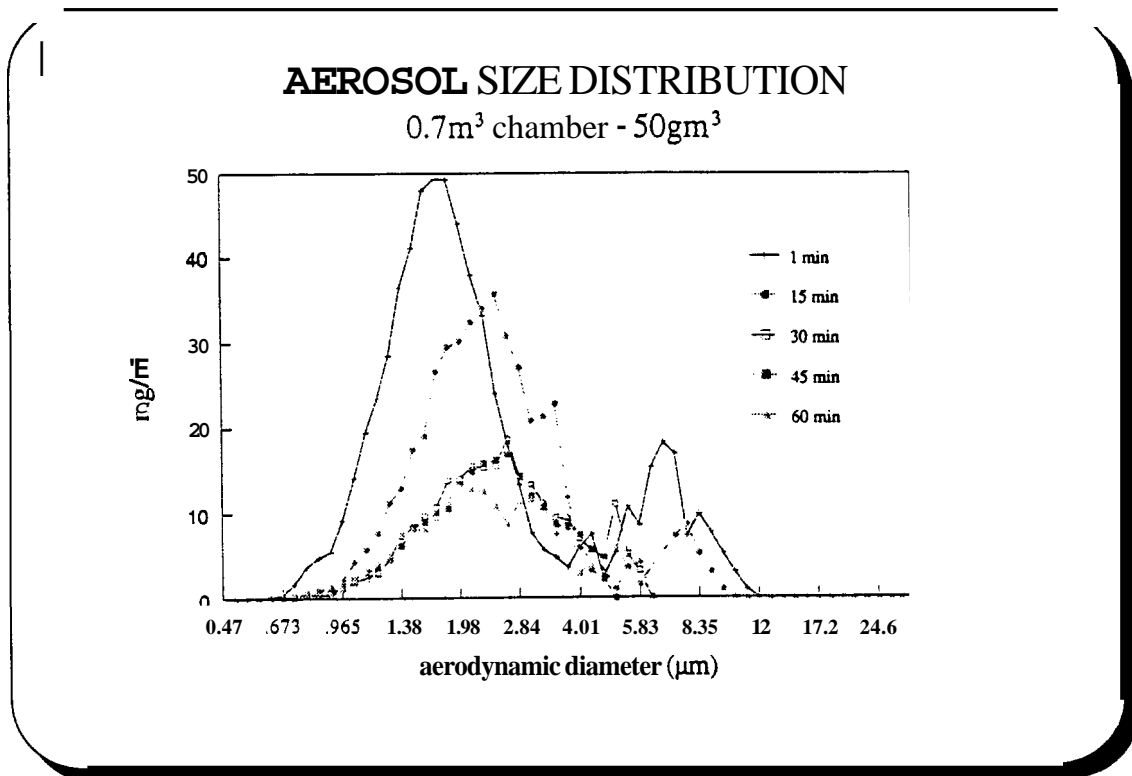
$0.7m^3$ chamber - $80gm^3$

Figure 5a. Aerosol Size Distribution - $0.7m^3$ chamber

AEROSOL SIZE DISTRIBUTION

56m³ chamber - 50gm³

AEROSOL SIZE DISTRIBUTION
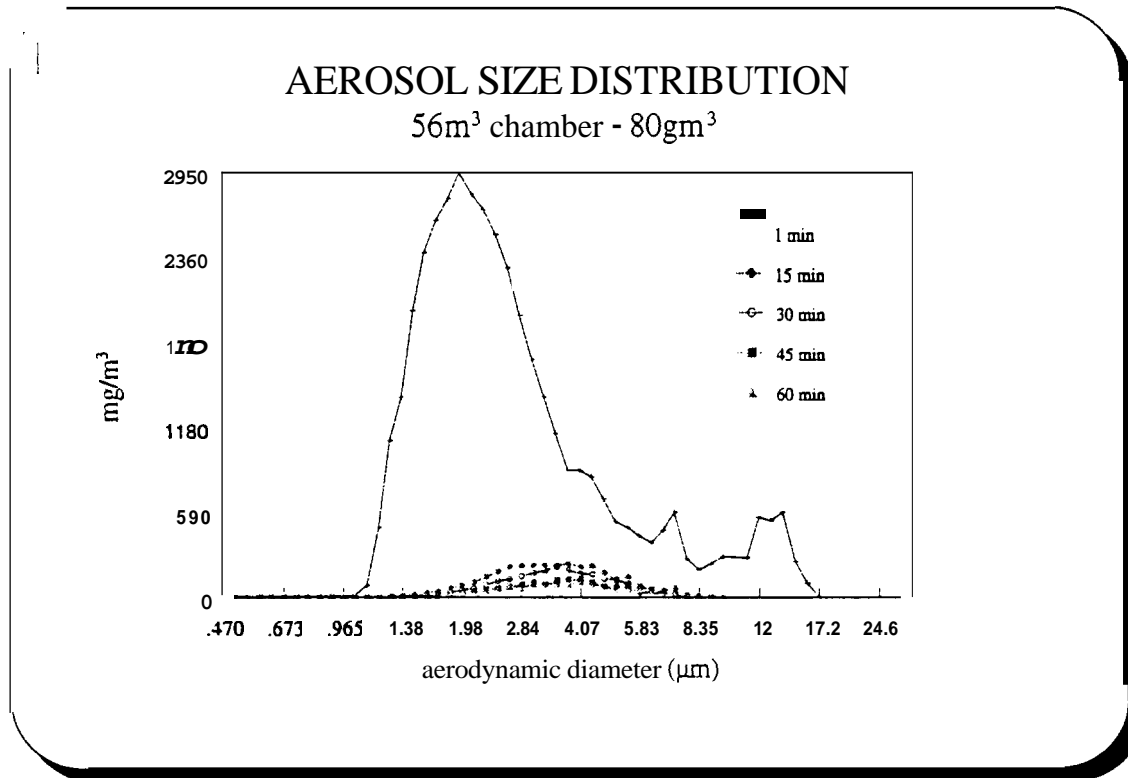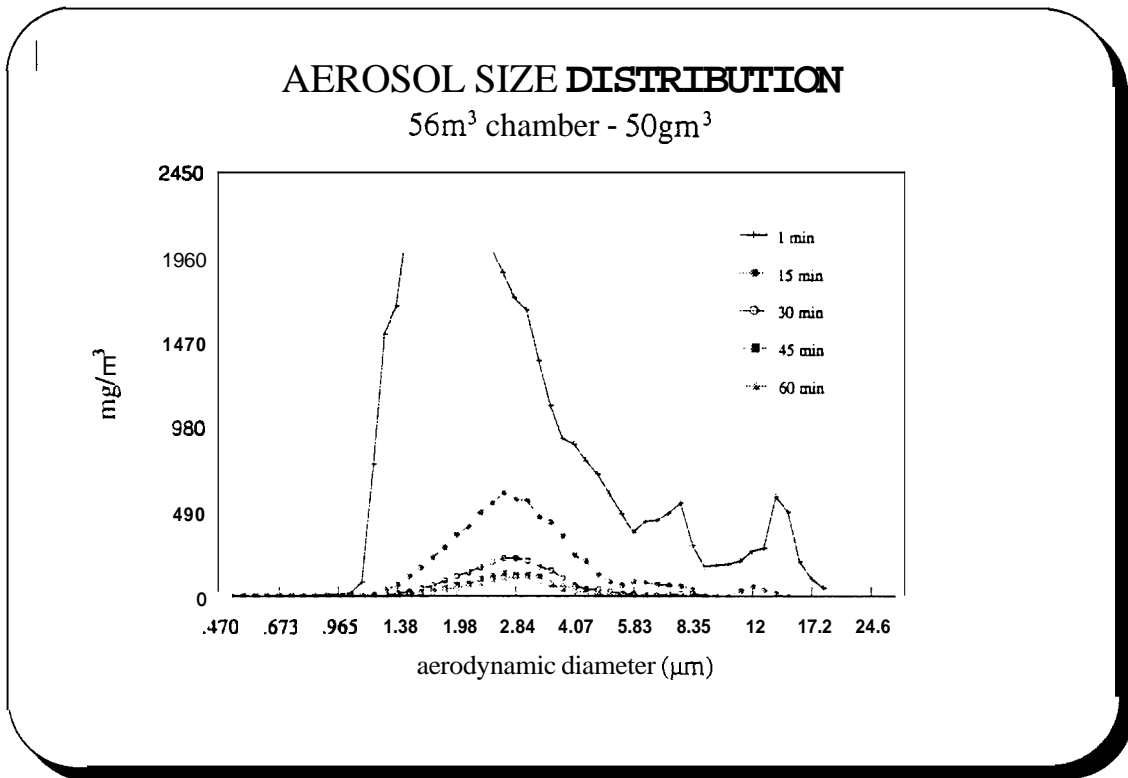
56m³ chamber - 80gm³

Figure 5b. Aerosol Size Distribution - 56m³ chamber
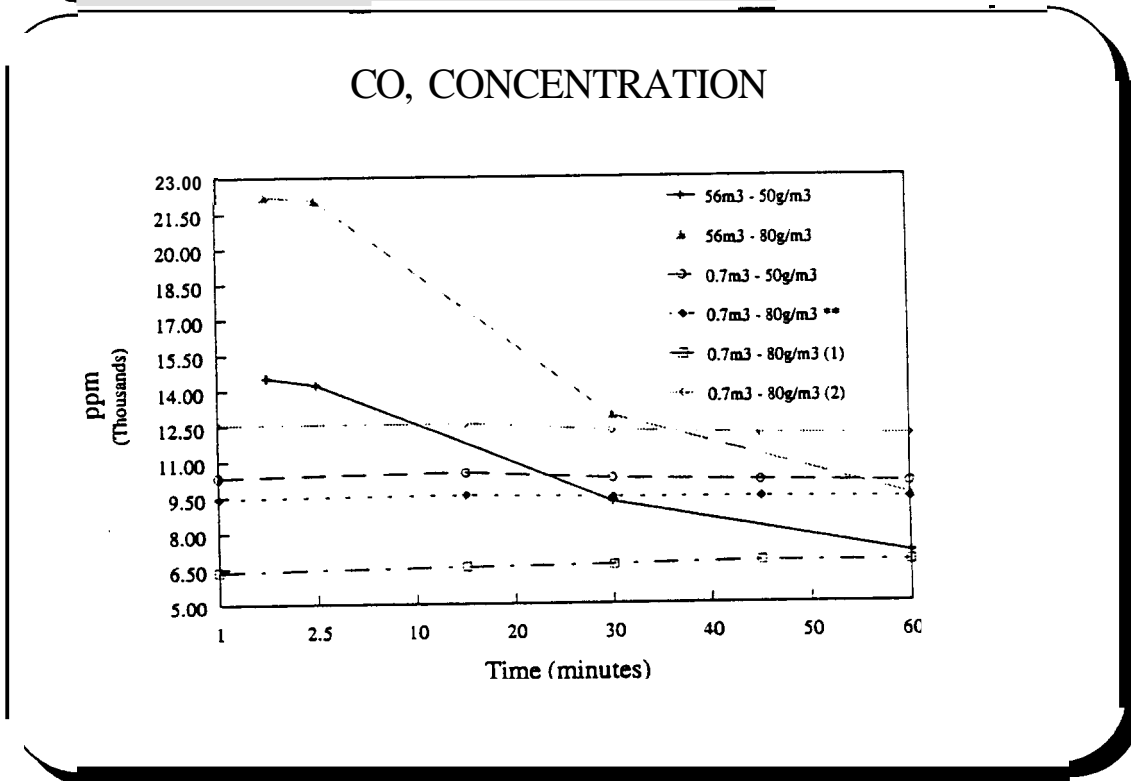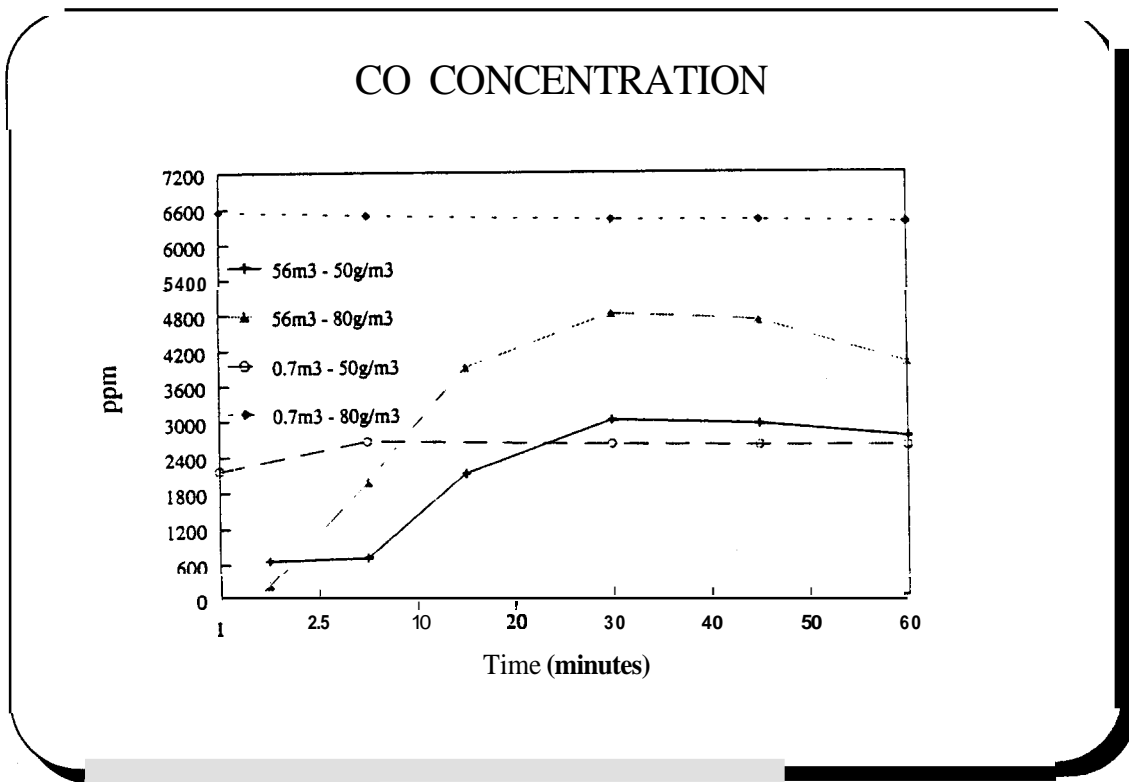
Figure 6. CO and CO₂ Concentrations

MASS BALANCE

$0.7m^3 - 50g/m^3$

	SFE	USED	AEROSOL	CO_2	CO	?
grams	35.7	23.9	4.4	13.5	2.2	3.9
%		66.9	12.3	38.2	5.9	10.7
g/m3			6.3	19.6	3.1	

MASS BALANCE

$0.7m^3 - 80g/m^3$

	SFE	USED	AEROSOL	CO_2	CO	?
grams	56.1	38.3	7	12.5	5.4	13.4
%		68.1	12.4	21.8	9.5	23.4
g/m3			10	17.8	7 8	
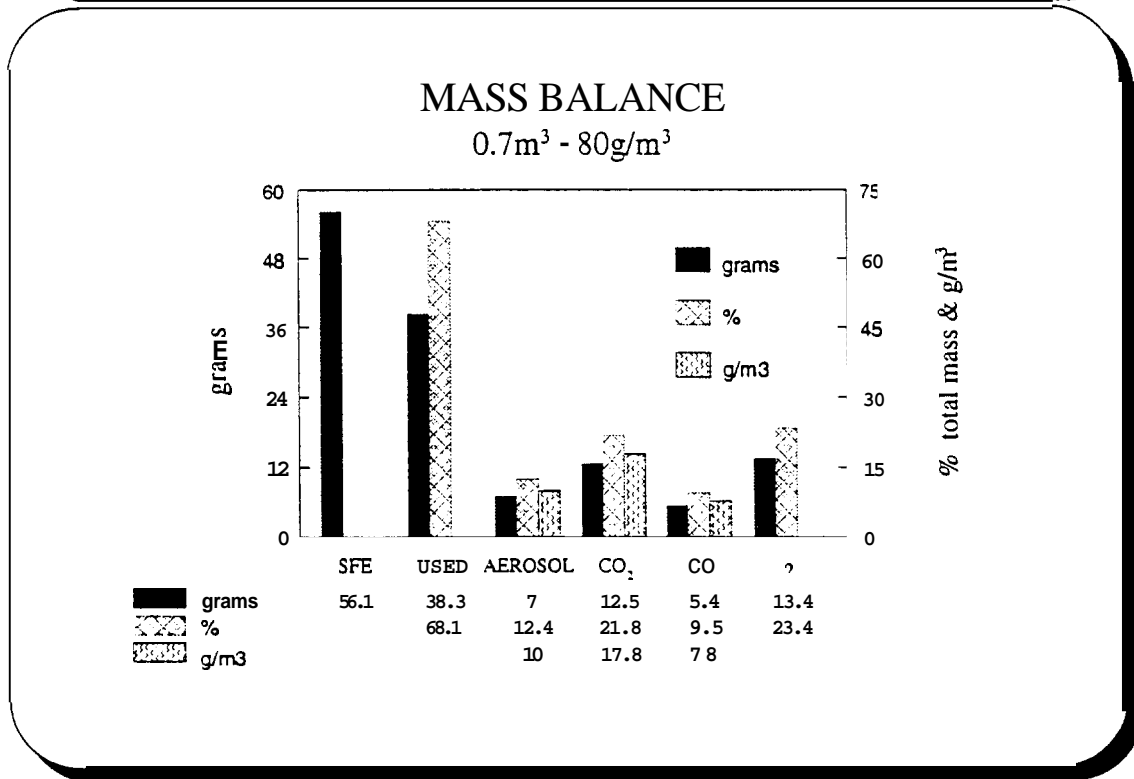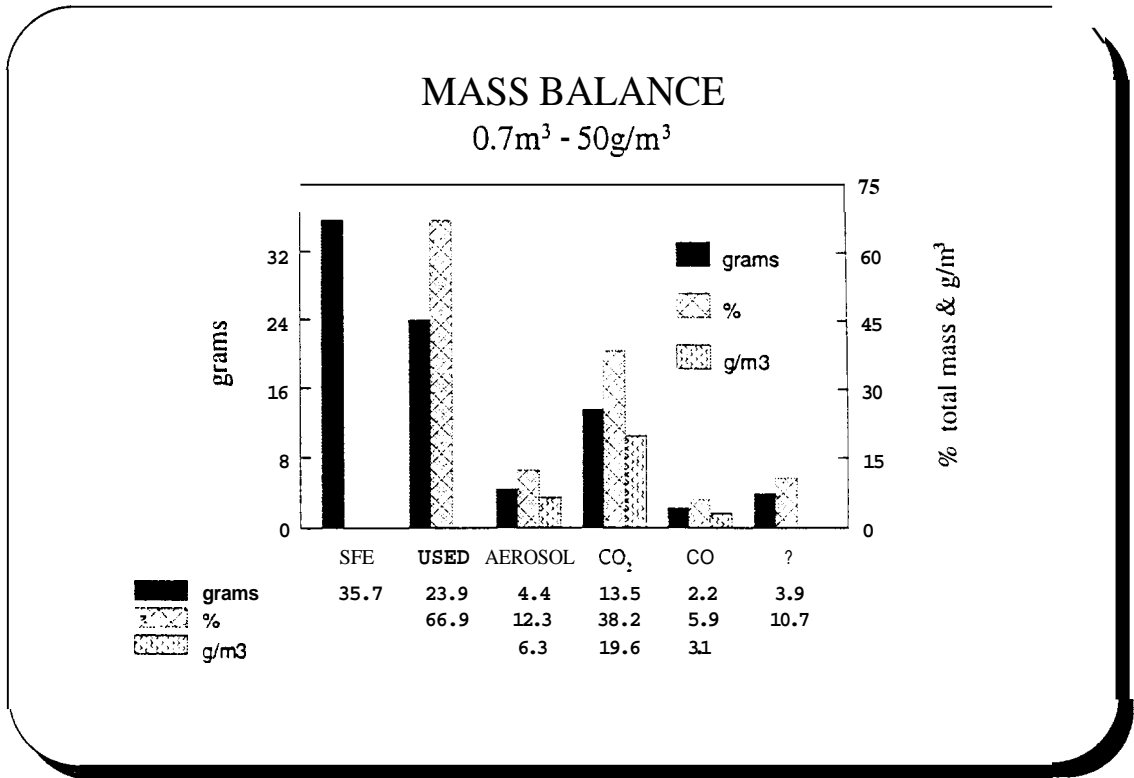
Figure 7a. Mass Balance - $0.7m^3$ chamber

MASS BALANCE'
56m³ - 50g/m³

	SFE	USED	AEROSOL	CO₂	CO	?
grams	3000	?	571	1489	194	746
%		?	19	49.6	6.5	24.8
g/m3			10.2	26.5	3.5	

MASS BALANCE
56m³ - 80g/m³

	SFE	USED	AEROSOL	CO₂	CO	?
grams	4500	?	704	2275	313	1128
%		?	17.4	50.6	6.9	25
g/m3			14	40.6	5.6	
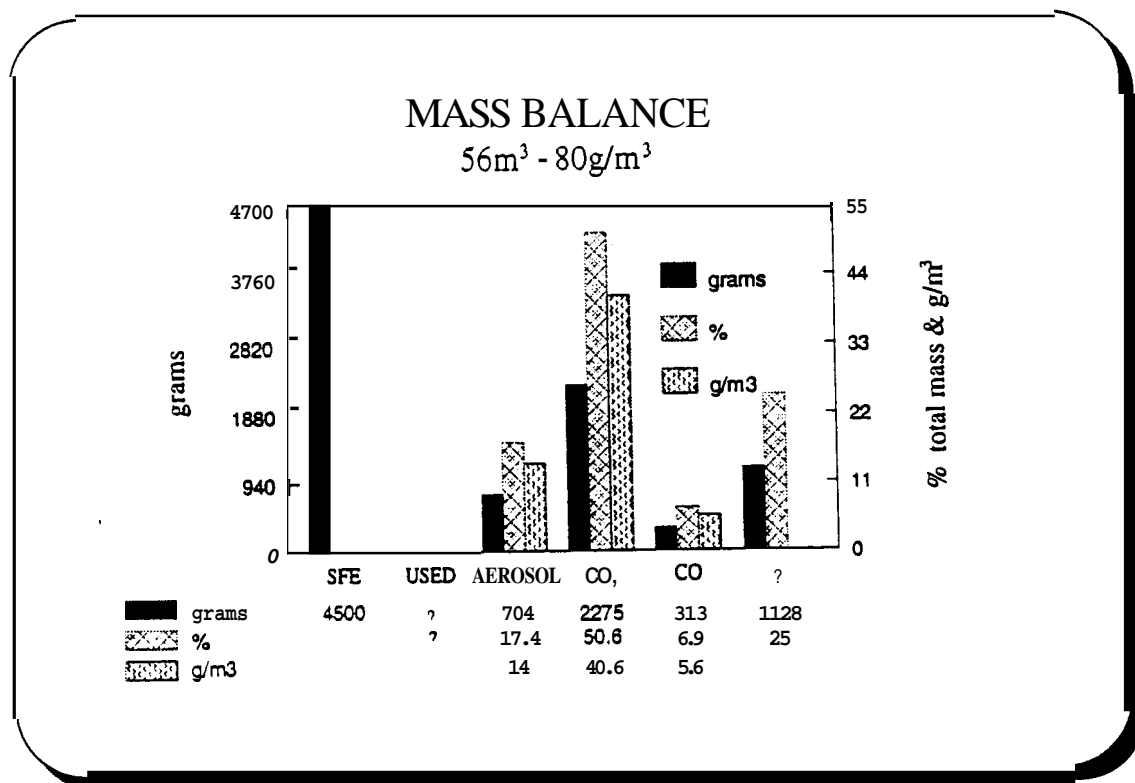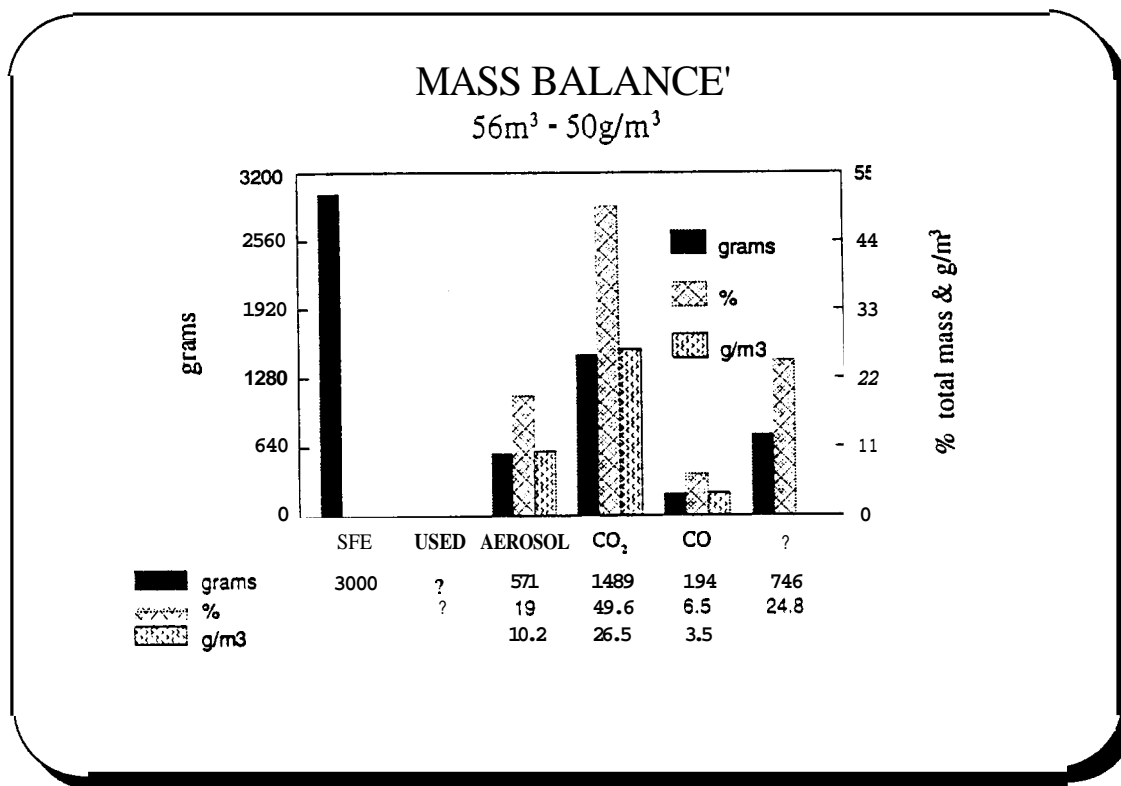
Figure 7b . Mass Balance - 56m³ chamber
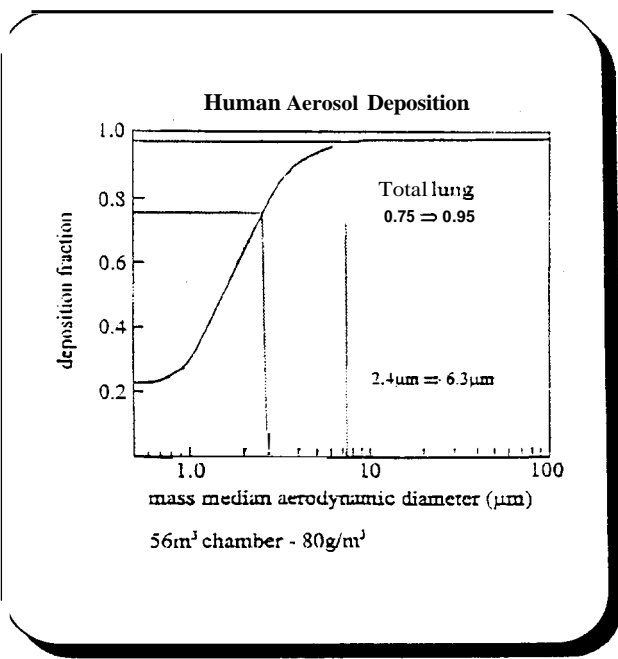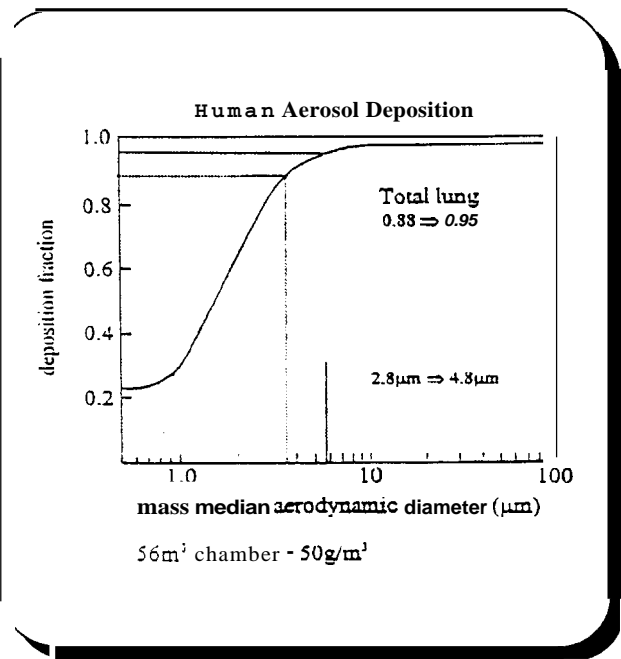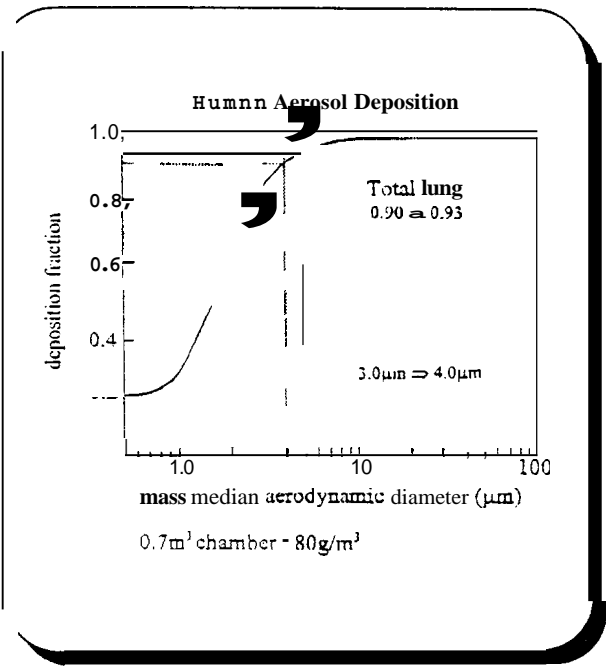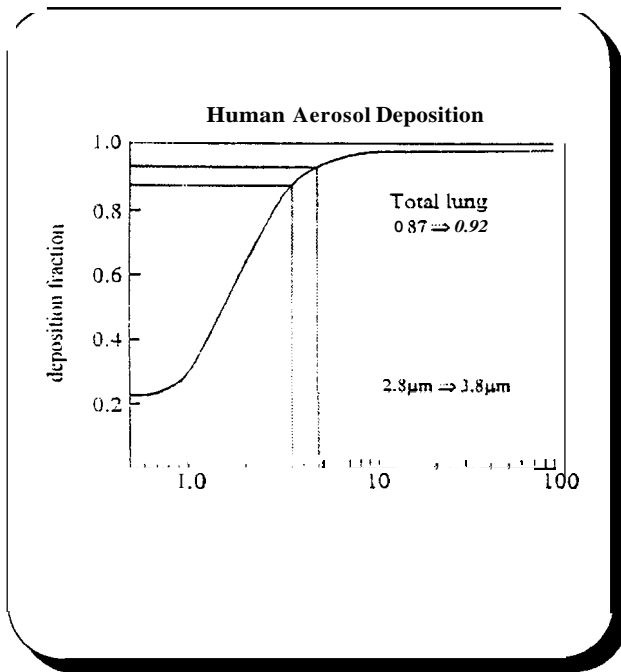
Figure 8. Total Lung Deposition
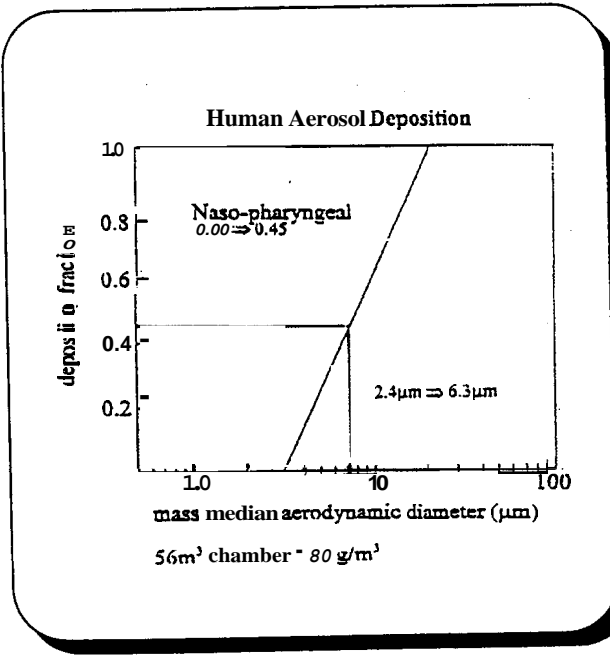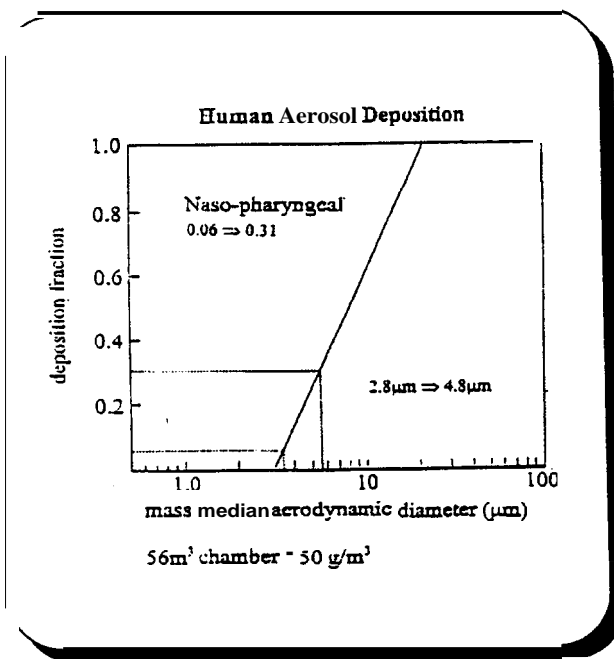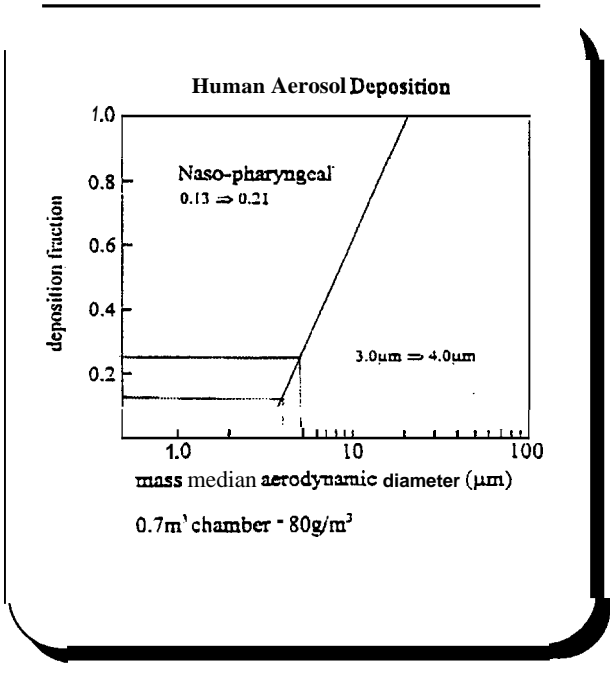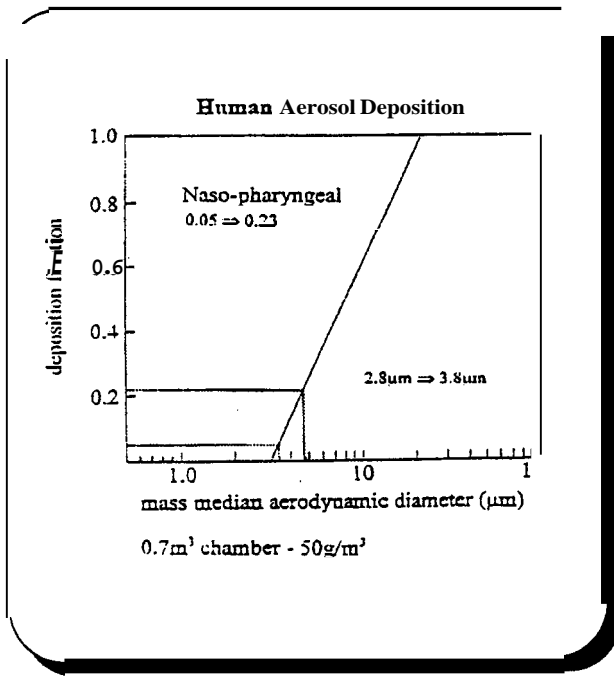
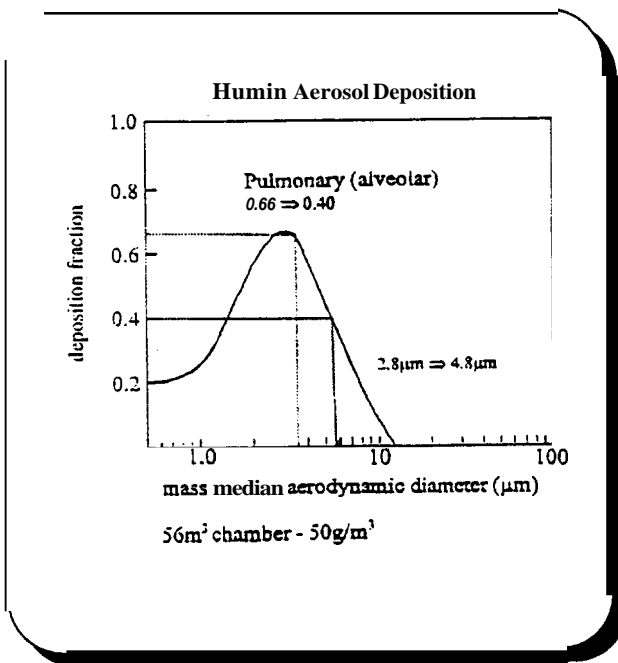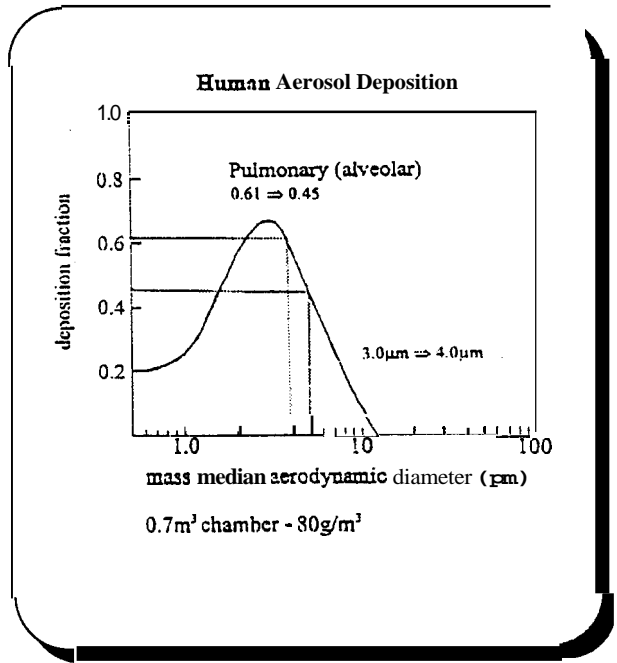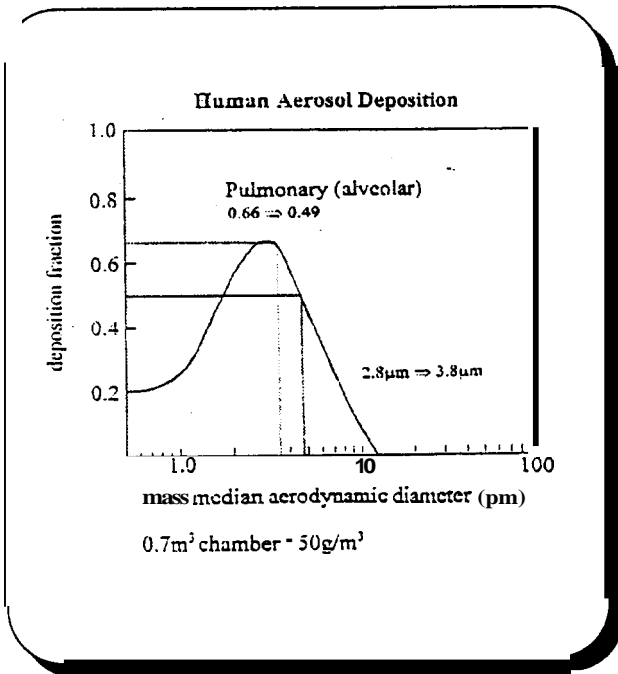Figure 9. Naso-oro-pharyngeal Deposition
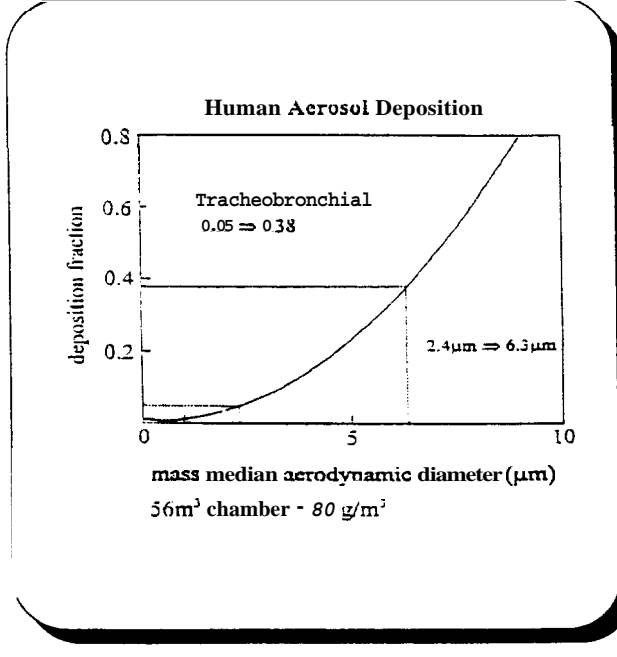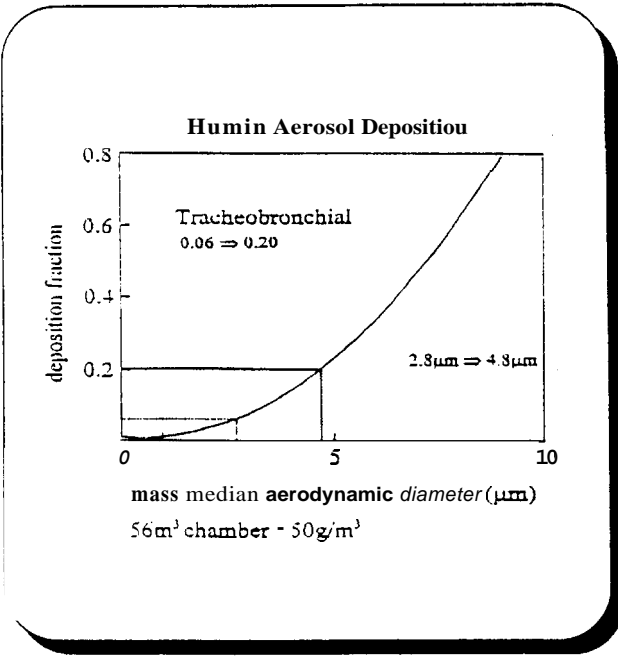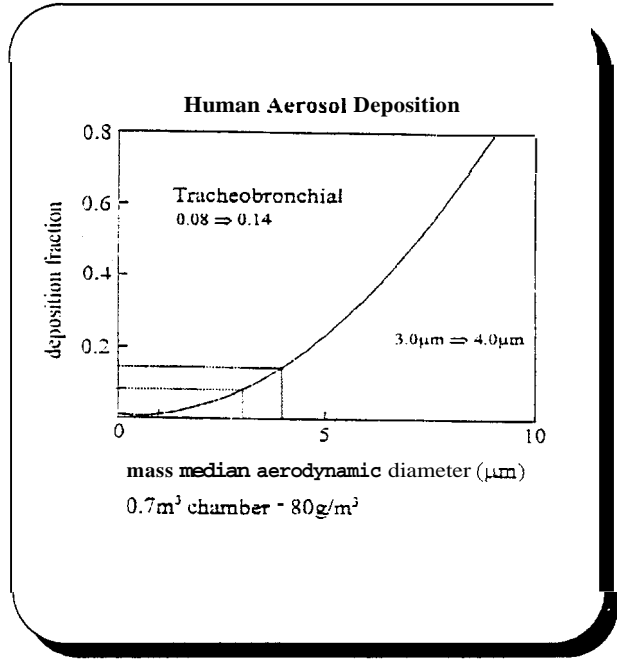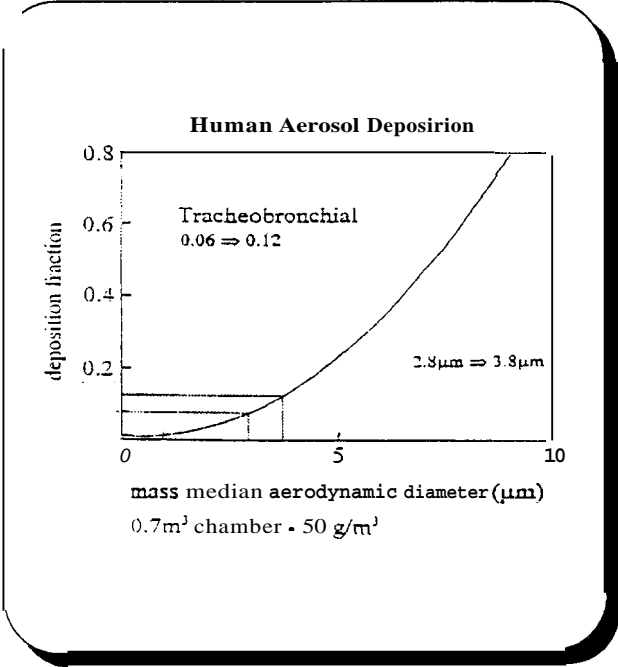
Figure 10. Tracheobronchal Deposition
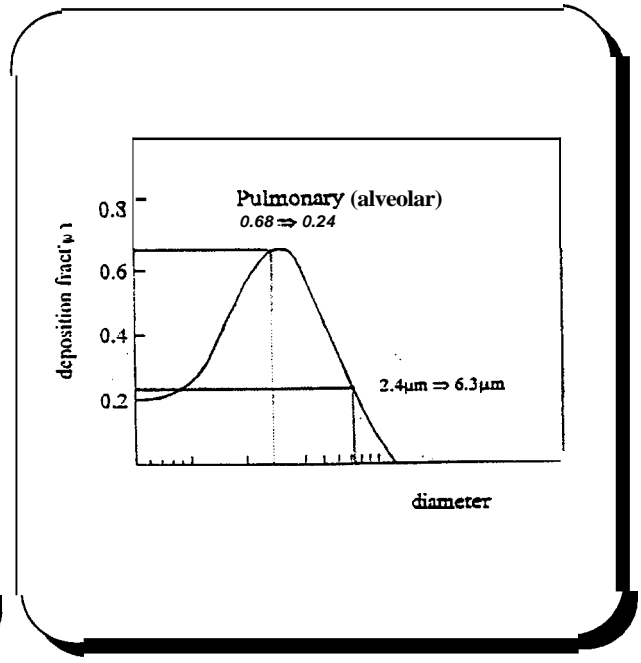
Figure 11. Pulmonary (Alveolar) Deposition